METEC & 6TH ESTAD 2023

Hydrogen-resistant refractories for direct reduced iron production

Milena Ribeiro Gomes[1], Antoine Ducastel[1], Lukas Konrad[1], Taco Janssen[2], Erick Estrada Ospino[3]

[1] RHI Magnesita, Magnesitstraße 2, 8700 Leoben, Austria
[2] RHI Magnesita, Clock Court, Campbell Way, Sheffield, United Kingdom, S25 3QD
[3] RHI Magnesita, 490 Elgin Street, Brantford, Ontario, Canada, N3S 7P8

Summary

In the steelmaking industry, the largest share of CO_2 emissions comes from the reduction of iron ore. A switch from the blast furnace (BF) / basic oxygen furnace (BOF) route to the direct reduced iron (DRI) process with natural gas followed by the electric arc furnace (EAF) already enables CO_2 savings of up to 38%. However, in order to meet the mid- to long-term CO_2 targets of the iron and steel industry, further measures are required. Most DRI plants are currently operating on natural gas, which results in approximately 60% hydrogen in the process gas. However, currently projects are underway to determine if DRI units can operate at hydrogen levels at or close to 100%, which could further reduce CO_2 emissions by more than 80%.

In this context, it is important to consider the impact of hydrogen on the refractory lining in the DRI shaft kiln. Previous studies have shown that hydrogen can permeate through refractories and reduce ceramic oxides under certain process conditions. Silica-containing materials are reported to be especially susceptible to hydrogen attack. However, a deeper understanding of corrosion mechanisms is still needed.

This article presents the first results of experimental work carried out by RHI Magnesita on the impact of hydrogen on refractory systems. Investigations were conducted on the effect of hydrogen exposure on the composition and microstructure of refractory bricks. This enables refractories to be identified that are suitable for lining a DRI shaft kiln where hydrogen is used as a reductant and will support the development of novel hydrogen-resistant refractory solutions.

Keywords: hydrogen, DRI, corrosion of refractory, alumina-silica bricks, oxide reduction, sustainable ironmaking, green steel.

1. Introduction

While steel responds for approximately 7% of anthropogenic CO_2 emissions worldwide [1], net-zero pledges from major players attest to the commitment of the industry to help forge a sustainable future, and new technologies have arisen and are being developed that could enable steel to be produced in a CO_2-free way.

Among them, hydrogen-based DRI stands out as a very promising solution. DRI is a proven technology that has been successfully operating for decades as an alternative to the BF/BOF route for the reduction of iron ore, using for the most part natural gas as a reducing agent. Now hydrogen is gaining attention as an alternative to natural gas which could push emissions down to even lower levels [2].

One of the attendant challenges of using hydrogen as the reducing agent in the DRI process is the implications it will have for the refractory lining. Silica has been demonstrated to be prone to hydrogen corrosion: it will react with H_2 to form volatile SiO as the main product (Eq.1). This has led to degradation of the refractory lining in reformer vessels, and in addition to that silicon monoxide may solidify downstream when it cools down, leading to the formation of deposits that can cause clogging, fouling and product contamination [3]. On the other hand, alumina has been demonstrated to have outstanding resistance. The primary product of reduction is aluminum in the gas phase (Eq. 2), but the reaction will only take place at very high temperatures: Li et al exposed alumina to hydrogen at temperatures going up to 1800 °C, and no reaction was observed [4].

$$SiO_{2(s)} + H_{2(g)} \rightarrow SiO_{(g)} + H_2O_{(g)} \quad \text{Eq.1}$$

$$Al_2O_{3\,(s)} + 3H_{2(g)} \rightarrow 2\,Al_{(g)} + 3H_2O_{(g)} \quad \text{Eq. 2}$$

There is, however, a lack of studies on the topic, and the behavior of refractories under hydrogen atmospheres is not very well understood. In this context, this study aims to investigate the effect of hydrogen exposure on dense and lightweight refractory bricks with different alumina and silica contents. The materials are exposed to a 100% H_2 atmosphere, and to atmospheres containing 98% H_2 with 2% CO or 98% H_2 with 2% CO_2, at temperatures up to 1400 °C.

2. Materials and methods

In this study, six different commercial bricks are investigated. They are listed in Table 1. Bricks D1, D2 and D3 are dense, whereas L1, L2 and L3 consist of lightweight insulating bricks. The sequence D1, D2, D3 has a rising alumina and decreasing silica content, and the same applies for the L sequence. For the trials, the bricks were cut into bars with dimensions of 20 x 20 x 100 mm.

The experiments were carried out in an electrical furnace. The materials were exposed to an atmosphere of 100% H_2 at temperatures of 1000, 1200 and 1400 °C, and subsequently to atmospheres of 98% H_2 with 2% CO, and 98% H_2 with 2% CO_2, at 1000 °C. Exposure time was of 200 h, and the pressure was kept at 1 atm for all trials with continuous replenishment of H_2. Each material was analyzed in duplicate.

The samples were weighted before and after exposure to hydrogen, and the chemical composition of the bricks was determined by X-ray fluorescence (XRF). The loss on ignition was measured at 1025 °C according to the standard ISO 26845. The samples were also observed in the scanning electron microscope (SEM), and different points were selected for an energy dispersive X-ray (EDX) analysis.

Table 1 – Major oxide composition and bulk density of the bricks used in the study.

Brick	Description	Al_2O_3 (wt%)	SiO_2 (wt%)	Fe_2O_3 (wt%)	TiO_2 (wt%)	P_2O_5 (wt%)	Bulk density (g/cm^3)
D1	dense fireclay brick with ceramic bonding	43.1	52.0	1.38	1.48	0.45	2.23
D2	dense andalusite brick with ceramic bonding	59.4	38.6	0.98	0.34	0.04	2.52
D3	dense high alumina brick with ceramic bonding including phosphate binder	90.4	6.59	0.30	0.11	1.66	3.09
L1	lightweight brick type 40% Al_2O_3 with ceramic bonding	40.2	54.2	1.85	0.76	0.08	0.51
L2	lightweight brick type 65% Al_2O_3 with ceramic bonding	65.8	32.0	0.70	0.24	0.07	0.94
L3	lightweight brick type 90% Al_2O_3 with ceramic bonding	90.0	9.23	0.25	0.15	0.00	1.40

3. Results and discussion

3.1 Trials on a 100% H_2 atmosphere

An initial visual inspection of the samples showed a color change: the originally white, beige or earthy materials became light or dark grey. Even though the darkening varied for each material and exposure time, all samples underwent a color change (Fig. 1).

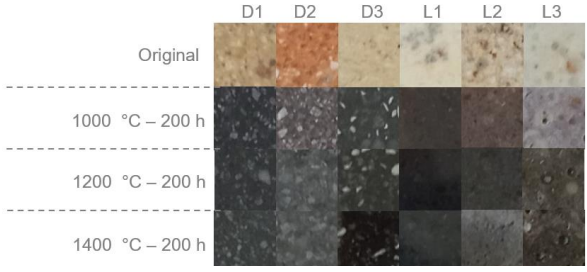

Figure 1 – Color change of the bricks after exposure to a 100% H_2 atmosphere at different temperatures. A color change to light or dark grey was seen in each case.

As the reduction of ceramic oxides by hydrogen usually generates gas-phase products, a decrease in weight is a reliable indicator that reduction took place. Figure

2 shows the weight loss of the refractory materials in a 100% H_2 atmosphere at 1000, 1200 and 1400 °C. The weight loss is low at 1000 °C, but becomes expressive at 1200 °C. The corrosion becomes more severe as the temperature increases, with brick L1 losing nearly 30% of its mass at 1400 °C.

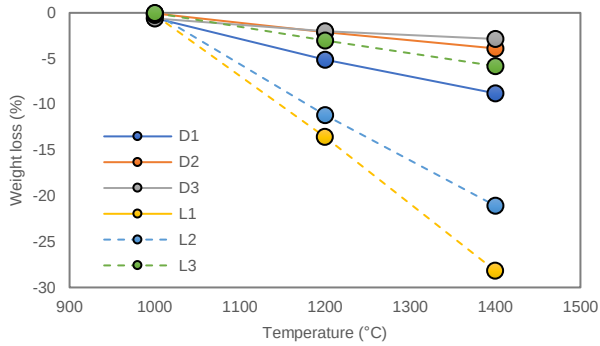

Figure 2 – Weight loss of the bricks after 200 h exposure to a 100% H_2 atmosphere.

A comparison between the samples clearly shows that weight loss is higher for the lightweight materials than for the dense bricks. This indicates that the reaction kinetics is dependent on mass transport. Hydrogen will more easily permeate the less dense materials and reach grain boundary and pore surfaces where it can adsorb and react with the oxides, while the reaction products will more readily find their way out from the interior of the bar to the gas stream in the furnace, allowing the reaction to proceed.

In addition to that, it can be seen that the higher the silica content, the higher the weight loss. Conversely, materials with a higher alumina content displayed a superior corrosion resistance. This trend can be seen for the dense as well as the lightweight bricks, among which D3 and L3 had the lowest weight loss respectively. The best performance was that of sample D3: the dense brick with the highest alumina and lowest silica content.

The analysis of the chemical composition of the samples shows depletion of silica after reaction with hydrogen (Fig. 3a). This confirms that the weight losses observed in Figure 2 at 1200 and 1400 °C can be mainly attributed to the reduction of silica, which will be removed from the sample in the form of SiO gas as described in Equation 1. On the other hand, alumina will not react in these conditions, and its proportion in the material will hence increase (Fig. 3b). This causes the A/S ratio to shift to higher values. At 1000 °C, however, the slight weight losses measured (of up to 0.64%) cannot be linked to the volatilization of silica. It can therefore be concluded that the onset of silica reduction by hydrogen is situated somewhere between 1000 and 1200 °C, or that if it happens at all at 1000 °C it is extremely slow-paced.

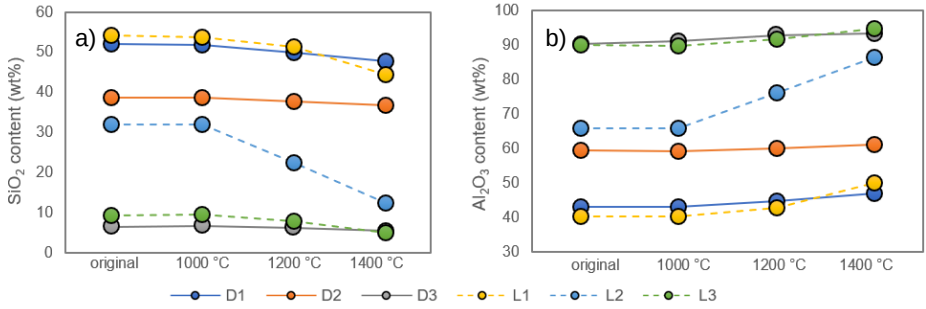

Figure 3 – Change in the relative silica (a) and alumina (b) content for each brick after exposure to a 100% H_2 atmosphere for 200 h.

The LOI of the materials can be seen on Table 2. For the most part, it became negative after hydrogen treatment: the samples gained weight when exposed to oxygen. This can be interpreted as the reoxidation of species that had been previously reduced under hydrogen atmosphere. As the products of reduction of silica are known to be in the gas phase, the weight gain should be associated with the reoxidation of impurities which form solid products when reduced, such as Fe_2O_3 (which will form metallic Fe). This is consistent with the fact that the samples with the most negative LOI values (D1 and L1) are those with the highest Fe_2O_3 content.

Table 2 – LOI of the bricks exposed to a 100% H_2 atmosphere for 200 h.

	LOI (%)			
	Original	1000 °C	1200 °C	1400 °C
D1	0.2	-0.26	-0.68	-0.62
D2	0.12	-0.03	-0.24	-0.08
D3	0.04	-0.08	-0.09	-0.05
L1	0.26	-0.29	-0.48	-0.62
L2	0.15	0.09	-0.04	0.01
L3	0.12	0.17	0.09	0.11

The observation of the microstructure of the exposed materials revealed interesting features. Droplets with a diameter of up to 1 µm (or slightly higher in the case of L1) were observed to form, as can be seen in Figure 4a. The droplets were found on all exposed samples starting from 1000 °C, their formation intensifying with increasing temperature. Their quantity also varied among the materials; sample L3, for instance, displayed only a very small number of droplets in all treatment temperatures. The beads were found to be located mainly at the pore surfaces in contact with the glassy matrix, but were also spotted at the rim of coarse grains.

EDX analyses allowed to identify that the droplets are comprised of Fe alloyed with a small amount of P and Si. The elemental composition of two droplets from sample D1 can be seen in Table 3. The presence of P shows that the phosphorous oxide

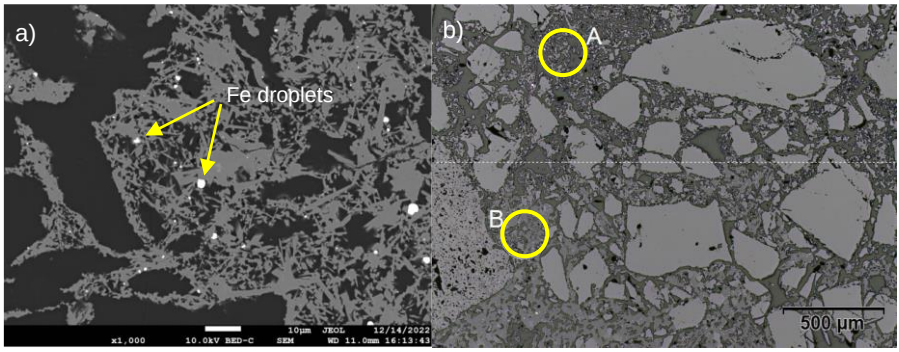

Figure 4 – a) Bright metal droplets in sample L1 after exposure to 100% H_2 flow at 1400 °C for 200 h; b) sample D3 after the same exposure conditions: in A, complete decomposition of mullite was observed with formation of secondary alumina, whereas in B residual mullite is present.

impurities were also reduced, and an accompanying depletion of P_2O_5 in the matrix of phosphate-bonded bricks was observed. The reduction of silica to Si metal is thermodynamically not expected to occur in the hydrogen-silica system [5] and it could be related to the presence of iron in this case, but this was not further investigated. The reduction of Fe_2O_3 and P_2O_5 impurities and subsequent formation of a metal alloy has been reported in the literature for bauxite castables as well [6]. It should be noted that the very small amount of Al shown in the elemental composition comes from the matrix, as the droplets are small and therefore difficult to isolate for analysis. Alumina was not reduced and Al was not present in the metal alloy. The incorporation of a matrix section together with the droplet is also the reason why some oxygen was detected.

Table 3 – Elemental composition obtained via EDX analysis of droplets formed in sample D1 after exposure to hydrogen flow at 1400 °C for 200 h. Al and O come from the matrix.

	Fe (%)	P (%)	Si (%)	Al (%)	O (%)
Droplet 1	94.8	0.4	0.9	1.2	2.5
Droplet 2	84.2	3.5	8.9	0.4	1.9

The reduction of iron oxide is behind the color changes illustrated in Figure 1. The EDX results also account for the negative LOI and the weight losses at 1000 °C: the slight decrease in weight is likely due to the loss of oxygen in the reduction of iron and phosphorous oxides to form the corresponding metals. As most of the iron impurities can be traced to the glassy phase, it explains the concentration of droplets on this region.

The SEM analyses also revealed the microstructural effects of silica reduction. In some of the samples the glassy phase was seen to decompose, and in the cases where the corrosion was more aggressive the mullite structure was also attacked. In samples D3, L2 and L3, the formation of secondary alumina was observed (Fig. 4b),

originating from the removal of SiO_2 from the glassy phase or mullite. Brick D3 showed secondary alumina formation in the fines up to 2 mm from the rim. The formation of secondary alumina has been reported in the literature [7], and in this study it was found to take place only when the A/S ratio is locally higher than 2.6 - a condition which can be reached earlier in bricks with a higher alumina content, but that can also be attained in materials which initially have less Al_2O_3 as silica is progressively removed.

Unexpectedly, the SEM analysis also revealed the formation of SiO_2 seams around fireclay grains at the rim of sample D1 (up to 8 mm) at 1400 °C. This is likely due to the reoxidation of SiO, but the origin of the oxygen needed for this is not clear to the authors.

3.2 Trials with 98% H_2 and 2% CO or 98% H_2 and 2% CO_2: comparison with 100% H_2 atmosphere

In addition to the tests under 100% hydrogen atmosphere, trials were also carried out with atmospheres containing 98% H_2 with 2% CO or CO_2 at 1000 °C. Those were motivated by FactSage simulations which indicated that those gases could affect the tendency of hydrogen to reduce ceramic oxides, even if present in very minor amounts in the gas stream [8]. However, as shown in Table 4, neither CO nor CO_2 bore an appreciable effect on weight loss at this temperature. Across the different trials, samples D2, L2 and L3 had a negligible weight loss, whereas samples D1, D3 and L1 had a small but significant weight loss. This is due to the presence of considerable amounts of iron impurities in D1 and L1, and to the phosphate binder phase in D3. Further chemical analyses and microstructural investigations also revealed no additional effect, except for a tendency to form less metal alloy droplets, slightly smaller in size and more finely dispersed.

Table 4 – Weight loss of the bricks exposed to different atmospheres at 1000 °C for 200 h.

	Weight loss (wt%)		
Material	100% H_2	98% H_2 + 2% CO	98% H_2 + 2% CO_2
D1	0.57	0.57	0.53
D2	0.07	0.06	0.08
D3	0.66	0.88	0.33
L1	0.22	0.09	0.36
L2	0.04	0.01	0.03
L3	0.02	0.03	0.07

4. Summary and conclusion

This study allowed to draw a comparison between different refractory bricks in terms of their corrosion resistance to hydrogen. Dense materials showed a superior performance compared with the lightweight bricks, and the resistance increased with

the alumina content and decreased with the silica content. Alumina remained unaffected by hydrogen exposure even at the highest temperature tested of 1400 °C, whereas silica reduction was clearly observed from 1200 °C. Silica was shown to be more easily attacked in the glassy phase than in the mullite grains. The removal of silica from either the glass or the mullite structure led to the formation of secondary alumina when the A/S ratio was locally higher than 2.6, or when it surpassed this value as a result of continuing silica removal. Besides silica reduction attended in some cases by the formation of secondary alumina, another change that was observed to be induced by hydrogen is the formation of metal droplets comprised of Fe with small quantities of alloyed P and Si, and for the most part concentrated on the interface of the pore surfaces with the glassy phase.

Based on these results, a recommendation can be made that the refractory lining in high-temperature applications with hydrogen-bearing atmospheres should have a high density and present a low silica content. Alumina, on the other hand, is likely a suitable lining material. Phosphate binders are easily reduced by hydrogen, and the content of glassy phase should be kept low as it is more susceptible to hydrogen attack. High aggregate purity levels are desirable, especially a low iron oxide content, even though the effect of impurity reduction and metal droplet formation on refractory properties requires further investigation.

5. References

[1] IEA, Iron and Steel Technology Roadmap, IEA, Paris (2020), https://www.iea.org/reports/iron-and-steel-technology-roadmap.

[2] Battlea T., Srivastavaa U., Kopfleb et al, The Direct Reduction of Iron, in: Seetharaman, S., Treatise on Process Metallurgy, 89-176 (2014), 3.

[3] Crowley, M. S. , Hydrogen-Silica Reactions in Refractories, Ceramic Bulletin 679-682 (1967), 46 [7].

[4] Li S., Chen D., Gu H., Huang A., Fu L., Investigation on Application Prospect of Refractories for Hydrogen Metallurgy: The Enlightenment from the Reaction between Commercial Brown Corundum and Hydrogen, Materials (2022), 15.

[5] Misra A. K., Thermodynamic analysis of chemical stability of ceramic materials in hydrogen-containing atmospheres at high temperatures (1990).

[6] Leber, T., Madeo S., Tonnesen T., Telle R., Corrosion of bauxite-based refractory castables and matrix components in hydrogen containing atmosphere, International Journal of Ceramic Engineering and Science 16-22 (2022), 4 [1].

[7] Herbell, T. P., Hull, D. R., Garg, A. Hot Hydrogen Exposure Degradation of the Strength of Mullite, Journal of the American Ceramic Society 910-916 (1998), 81 [4].

[8] Koncik, L. Thermodynamic modelling of H_2, H_2O, CO an C on common oxides used as refractory, RHI Magnesita internal report, 2022.

This project has received funding from the European Union's Horizon Europe research and innovation program under grant agreement no.101072625.